



Exploring micromechanical behaviors of soft rock joints through physical and DEM modeling

Hoang-Khanh Le¹ · Wen-Chao Huang¹ · Chih-Chun Chien^{1,2}

Received: 6 May 2020 / Accepted: 16 December 2020 / Published online: 15 January 2021
© Springer-Verlag GmbH Germany, part of Springer Nature 2021

Abstract

The joint surface of a rock mass is one of the most important factors that strongly affect its shear strength, which is critical in rock engineering. Specifically, the joint roughness coefficient (JRC) is a parameter that represents the profile characteristic of the joint. In the authors' earlier investigation, any joint profile with a given JRC might be generated randomly for engineering purposes. In this study, a series of direct shear tests in both laboratory and numerical modeling (through discrete element method (DEM)) was conducted for soft rock joints to elucidate the mechanical properties of a randomly-generated JRC profile. A 2D-DEM model was adopted to simulate the joint specimen under the same direct shear conditions as in the laboratory tests. A reasonable agreement is found between the experimental direct shear tests performed on an artificial gypsum plaster model and the numerical modeling that was carried out, showing that the numerical model can be used in the interpretation of the direct shear tests of joint surfaces. Besides, the peak shear strength of the gypsum model also compares well with that predicted by Barton's equation. Based on the lab test results and numerical simulation, the failure mechanism of the joint specimen is correlated with the normal stress applied. From a microscopic viewpoint, the distribution of contact forces is most concentrated at the early stage during shearing, especially at the time of the peak shear stress. The distribution of shear stresses along the shear plane is not uniform, depending on the degree of joint undulation. The peak shear strength of the soft rock joints mostly comes from the roughness along the joint surface. However, the residual strength is mobilized from reduced roughness and the shearing-off of the joints.

Keywords Joint roughness coefficient (JRC) · Joint shear strength · Direct shear simulation · Micromechanics · Discrete element method (DEM)

Introduction

The shear strength of rock mass containing discontinuities, such as joints and bedding planes, plays an essential role in estimating the stability of a rock slope and tunnels in rock engineering. For practical purposes, Barton (1973) developed an empirical equation (Eq. 1) for the peak shear strength of a joint, which has been commonly used for several decades. In Eq. 1, τ denotes the shear strength of the rock joint; σ_n denotes

the normal stress. JRC denotes the joint roughness coefficient, which was one of the most critical factors that influenced the shear strength of such a joint, JCS means the joint compressive strength, and ϕ_b denotes the basic friction angle.

$$\tau/\sigma_n = \tan \left[(JRC) \cdot \log_{10} \left(\frac{JCS}{\sigma_n} \right) + \phi_b \right] \quad (1)$$

In Barton's equation, the evaluation of the JRC might be subjective because the joint profile had to be visually compared with the standard profiles. Subsequently, more highly accurate approaches such as the root mean square (Myers 1962), the fractal dimension (Lee et al. 1990; Wakabayashi and Fukushima 1992), and the inclination fitting (Tatone and Grasselli 2010) for evaluating the JRC have been proposed. Each method for estimating the JRC showed different criteria and parameters which needed to be assessed. Various choices of approaches made the practitioner face with difficulty to decide which criterion was the most suitable amongst the

✉ Wen-Chao Huang
wenchao@g.nctu.edu.tw

¹ Department of Civil Engineering, National Central University, Taoyuan City 32001, Taiwan

² Department of Environmental Information and Engineering, Chung Cheng Institute of Technology, National Defense University, Taoyuan City 32001, Taiwan

existing ones. Therefore, a more straightforward method in assessing the roughness of a joint may be required for practical use.

Lê et al. (2018) proposed the use of the Profile Height Variation (PHV) method for generating any artificial joint profile with given JRC value. A series of direct shear (DS) simulations were then performed on models containing the artificial joint profile with $JRC = 19.6$. However, no laboratory test was conducted to compare with the numerical results. Besides, the smooth joint model, which was an advanced model for simulating the mechanical behavior of rock joint, was also not applied in their PFC-2D simulations. Therefore, the generation of an artificial specimen under a given JRC value may be required for laboratory testing. Le et al. (2019) applied the PHV method for printing out a joint block with $JRC = 19.6$ using 3D-printing technology. Conversely, their results were only based on the observation in the laboratory. A more detailed discussion about the mechanical behaviors may be required with the numerical simulation from the micromechanical point of view.

Therefore, this study focused on the comparison between physical and numerical modeling by performing a series of DS tests or simulations. The artificial rock joint profile with a given $JRC = 19.6$ was constructed using the PHV method (Lê et al. 2018). The same joint profile ($JRC = 19.6$) is used for casting the artificial gypsum specimen and for numerical simulation. In the laboratory, the joint block with $JRC = 19.6$ was produced indirectly using 3D-printing technology. The artificial joint specimen (gypsum plaster with quartz sands) was replicated based on the printed block. When the casting process was completed, artificial joint specimens were laser-scanned to determine the actual JRC of the joint, which was later used in a numerical model. The shear strength of the gypsum specimen obtained from the laboratory tests may be reexamined with that predicted by Barton's equation. The DS tests with the specified joint profile were modeled using a 2D circular rigid particle model (PFC-2D by Itasca Inc. 2017) based on the 2D discrete element method (2D-DEM), under the same conditions that applied in the laboratory. Once 2D-DEM models are validated with that of the laboratory tests, the micro-mechanical behaviors of the rock joint can be analyzed and discussed. The discussion of micromechanical behaviors includes the analysis of the contact force distribution between the particles, the percentage, and locations of the broken bonds between the particles. A more detailed discussion of the micromechanical behaviors is shown in a later section.

Literature review

The estimation on the shear strength and the JRC of a rock joint has been made by many researchers (Bandis et al. 1983; Jing et al. 1992; Klinkenberg 1994; Kana et al. 1996; Belem

et al. 2000; Pickering and Aydin 2016). Liu et al. (2017a, b) evaluated the JRC of a joint rock profile by estimating both first-order and second-order asperity of such a joint under DS conditions. Their test result on sandstone joints showed that the JRC, the normal stress level, and the thickness of an interlayer rock significantly affected the shear strength of the rock joint; however, the failure mechanism of the interlayer rock was not investigated in their study. Liu et al. (2017a, b) proposed a new peak shear strength model using many DS tests on jointed specimens with different surface morphologies. The authors also introduced a new functional relationship between the dip angle and the contact area of the joint surface, which correlated with the JRC. The equation in their study was constructed based on ten standard profiles, which might need to be checked with more realistic joint profiles. Besides, the failure mechanism of granite rock joints was also investigated based on many DS tests (Meng et al. 2018). The results indicated that the roughness of the discontinuity plane and the micro-texture of host rock both affected the stability of fault slip.

Besides, the characteristic of rock joints was also evaluated using numerical modeling comprising the finite element method (FEM), the finite difference method (FDM), and the discrete element method (DEM). Liu et al. (2014) investigated the influence of the model parameters, including the JRC and the JCS on the shear strength of rock joints. A series of unconfined compression strength (UCS) tests and DS tests were simulated using FLAC3D coupling with Mohr-Coulomb models. The results indicated that the increase of the cohesion, internal friction angle, and the shear strength of the joint surface was associated with the rise of the JRC. The authors emphasized that the JRC and JCS both contributed to the shear strength of a rock joint. However, the influence of the JRC was more significant than that of the JCS. Fan et al. (2015) proposed the use of a 3D rigid spherical particle model based on the 3D discrete element method (PFC-3D by Itasca Inc.) for estimating the mechanical properties of multi-non-persistent rock joints under uniaxial loading. Their results presented that the UCS of the joint specimen strongly depended on the joint inclination angle and the joint continuity factor. Huang et al. (2015) used the 2D-DEM model to explore the micromechanical behavior of particle assembly under direct shear conditions. The numerical results showed that the stress path variations and the orientation of the major principal stress plane were highly influenced by compaction states of the granular materials. Cheng et al. (2016) also adopted the DEM for evaluating the mechanical behaviors of the rock mass, such as strength mobilization, the mechanism of damage, and the joint geometry under uniaxial compression conditions. Wang et al. (2017) carried out a large number of DS tests using different discrete fracture network (DFN) models, which aimed to estimate the complex geometry and the directionality of the fractured rock masses. Their results

showed that the shear strength of simulated rock was associated with the orientations of the fracture relative to the loading direction. The abovementioned research works have shown that DEM can be successfully used to study the mechanical behavior of a jointed rock mass or geotechnical materials. Conversely, most of the previous studies did not compare the results between laboratory tests and numerical simulations, especially the micromechanical behavior of a joint surface during shearing has not been investigated.

Additionally, Le et al. (2018) collected 86 actual joint profiles from published studies for evaluating the properties of the JRC. The results from statistical analysis proved that the JRC value of any rock joint profile could be determined based on the relationship between the JRC and the standard deviation (σ_{PHV}) of the profile height variation (PHV) of such a joint (Eq. 2). PHV was defined as the profile height difference for the adjacent sampling points on the joint profiles. A new method, which based on the zero mean value and the standard deviation of the PHV, was then presented to produce a joint profile with a particular JRC. Subsequently, any number of PHV following the above statistical parameters with an assumption of the normal distribution could be created for further applications. For example, a rock joint profile with a length of 10 cm could be constructed by adding up 400 data points (399 PHVs) one after the other with a fixed segment length of 0.25 mm along the horizontal axis and a starting point at zero elevation. Figure 1 illustrates three randomly generated profiles with JRC = 10, JRC = 19.6, and JRC = 20 as examples. One could see a distinct variation of the profiles for small and large JRCs. Therefore, any artificial JRC profile with a given JRC value could be artificially generated using the above approach. Lê et al. (2018) also produced and calculated 1000 randomly generated JRC profiles using existing

estimation approaches. They found that each estimation method yielded different comparison results, and JRC values estimated by the root mean square method (Myers 1962) compared well with the given JRC values. Subsequently, they adopted PFC-2D to simulate the rock joint with the above JRC profile (JRC = 19.6) under DS conditions. Their results indicated that normal stress levels strongly influenced the peak shear strength of the joint model. However, this conclusion may need to be compared with the lab test result to check the validity of the above PHV method.

$$\sigma_{PHV} = 0.0277 \exp(0.0687JRC) \quad (2)$$

Le et al. (2019) applied the above PHV method of the JRC profile to print out a joint block with JRC = 19.6 using 3D-printing technology. The joint blocks, including the lower and upper parts, were then used to replicate an artificially-jointed specimen with the same JRC using a gypsum mixture for direct shear tests. All specimens were sheared under different normal stresses of 0.4 MPa, 1 MPa, and 2 MPa. The test result indicated that the shear strength of the artificial joint specimen and the failure mechanism of the joint profile strongly depended on the normal stress applied to the specimen, which was based on the stress-strain curve and the observation of the joint surface after the test. Under low normal stress, the shear strength of the gypsum specimen mostly came from the frictional property along the joint surface. On the other hand, both friction and cohesion contributed to the shear strength of the specimen under intermediate normal stresses. Under high normal stress, the shear strength mostly arose from the cohesion. These findings provide us more understandings of the complex mechanical behavior of rock mass containing joints. However, in their study, the comparison in the peak shear

Fig. 1 Randomly generated joint profiles: (a) JRC = 10, (b) JRC = 19.6, and (c) JRC = 20

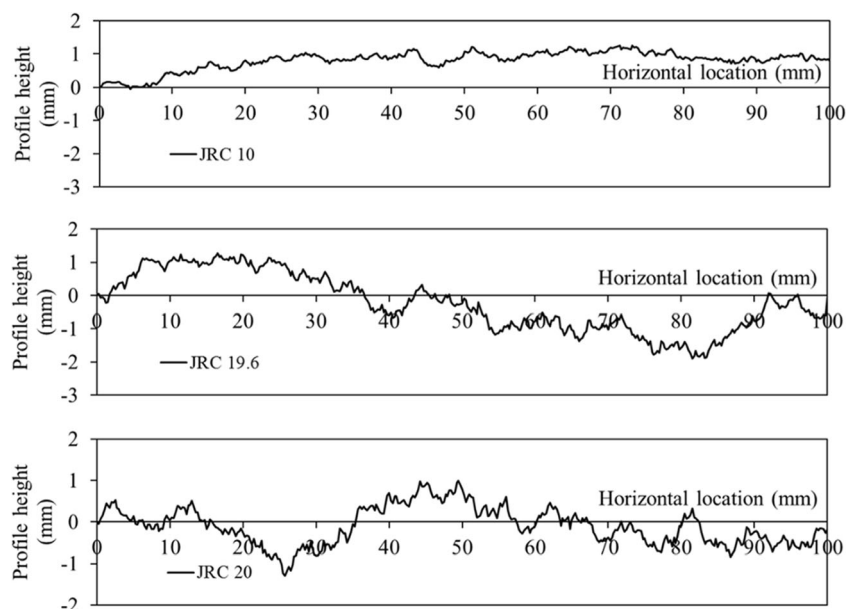
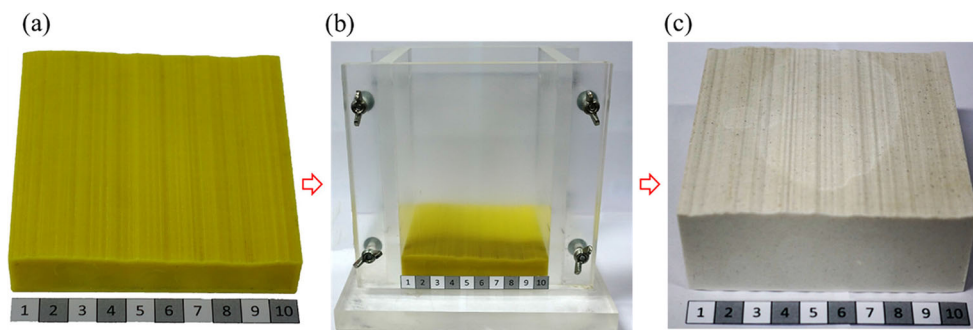


Fig. 2 The casting process of an artificial specimen: (a) the 3D-printed block with JRC = 19.6; (b) the acrylic box; (c) the complete artificial joint specimen



strength of the artificial joint specimens between the laboratory tests and Barton’s equation still needs to be revisited. The gypsum specimen under the normal stress of 2 MPa was broken into two pieces during shearing. The reason might be due to the non-uniformity of artificial gypsum specimens during the replicating process and the inadequate quality in the curing environment. Besides, visual observations on the characteristic of the joint may need to be checked with the numerical simulation from a micromechanical viewpoint.

Methodology

Laboratory test and the results

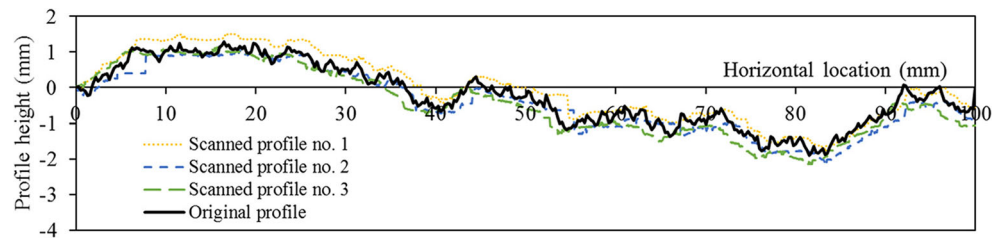
In this study, three unconfined compression strength (UCS) tests were performed to determine the average compressive strength of the gypsum mixture, which was the same mixing ratio of the jointed specimen. The mixture ratio of gypsum, quartz sand, and water was 1:0.75:1 by weight. The height (H) and diameter (D) of three cylindrical specimens were 125 mm and 50 mm, respectively. The H/D ratio of the specimen was about 2.5:1, which satisfied the requirement suggested by ASTM (2~2.5) and ISRM (2.5~3). The average UCS of the gypsum mixture was approximately 4.42 MPa, and this value was later used to calculate the peak shear strength of the jointed specimen using Barton’s formula. Besides, the UCS of the gypsum specimen also indicates that the specimen is a soft artificial rock specimen. The UCS was equivalent to the JCS

because the rock mass was assumed to be un-weathered. In the DS test, the 3D-printed jointed block with JRC = 19.6 was employed to replicate the lower and upper parts of an artificial joint specimen, which based on the PHV method and 3D-printing technology. With an identical profile property of JRC = 19.6, the improvement of test results in the current study can be observed and compare with the result of Lê et al. 2018, Le et al. 2019). In the laboratory, the joint specimen with a particular JRC value was replicated as the following steps (Fig. 2). Firstly, the 3D-printed jointed block (Fig. 2a) was located in the acrylic box (Fig. 2b), with dimensions 10 cm by 10 cm by 15 cm. The box was used as a mold for casting an artificial specimen. The connection between the printed block and the walls of the acrylic box should be tight enough to avoid the leaking of gypsum mixture from the box. Secondly, the artificially jointed specimen was replicated by gradually pouring the raw material with three layers into the mold; the thickness of each layer was about 1.2 cm. Once each layer had been poured, the acrylic box was then shaken at a given frequency for 1 min to expel all bubbles from the gypsum mixture. When the pouring process of three layers was completed, a waiting time of 1 h was required to solidify the mixture. Afterward, the complete casting specimen (Fig. 2c) was detached from the acrylic box and was cured in a moisture-controlled cabinet for 7 days before testing. The moisture and the temperature inside the cabinet were controlled as 50% and 26 °C. A similar procedure was applied to cast the lower and upper parts of an artificial joint specimen for direct shear tests. As a result, the lower part could be fully

Table 1 Comparisons on the peak shear strength amongst lab tests, Barton’s formula, and 2D-DEM simulation

Normal stress (MPa)	Peak shear strength				
	Laboratory test (MPa)	Barton’s equation (1973) (MPa)	Percentage difference between the lab test and Barton’s equation (%)	2D-DEM simulation (MPa)	Percentage difference between the lab test and 2D-DEM simulation (%)
0.400	0.560	0.572	- 2.075	0.650	- 13.846
1.000	1.135	1.124	0.972	1.125	0.889
2.000	1.820	1.884	- 3.385	1.867	- 2.517

Fig. 3 The scanned profile of gypsum specimen with JRC = 16.8 and the comparison with the given initially profile (JRC = 19.6)



combined with the upper part to form a joint specimen with the given JRC value.

The joint profiles of all gypsum specimens after replicating were also laser-scanned and recalculated to determine the actual JRC value. The scanning result of the artificial joint surface was plotted and compared with the originally given JRC profile, as illustrated in Fig. 3. The JRC value of the joint profile with JRC = 19.6 (original value) was recalculated using root mean square method (Myers 1962) and normal distribution method (Le et al. 2018) as 16.8. The calculation result indicated that the JRC value of the artificial specimen was slightly reduced after replicating from the printed joint block. The reason for this reduction might be due to the casting process, and the printing quality of the joint blocks such as the heating temperatures, the printing direction, and the thickness of the printing layer (Fereshtenejad and Song 2016). The length, the width, and the height of the DS specimen were 100 mm, 100 mm, and 70 mm, respectively. The DS test was conducted under the normal stresses of 0.4 MPa, 1 MPa, and 2 MPa at a constant velocity of 0.5 mm/min. The test was terminated when the total shear displacement of 10 mm or peak strength was reached. As mentioned previously, the actual JRC value of the joint profile was determined as 16.8. The basic friction angle of gypsum specimens was obtained as 37.5° , which was based on the DS test of flat jointed gypsum specimens in this study. Figure 4 shows the test result of the flat surface model and the determination of the basic friction angle. With a known UCS of the material and known normal stress, the peak shear strength of a particular joint

specimen could be calculated using Barton's formula. The calculation result of the peak shear strength of gypsum specimens under different normal stresses was shown and compared with the result of the lab test (Table 1). The difference in the peak shear strength between the lab test and Barton's formula was evaluated by calculating the value of the percentage difference. The positive value of the percentage difference indicates that the shear strength obtained from the lab test is higher than that calculated from Barton's formula. In contrast, the negative value shows a reverse trend. The results of shear stress versus shear displacement for gypsum specimens are also plotted in Fig. 5. The peak shear strengths of three artificial specimens (0.56 MPa, 1.135 MPa, and 1.82 MPa) under different normal stresses (0.4 MPa, 1 MPa, and 2 MPa) were reached at the shear displacements of 1.8 mm, 3 mm, and 2.8 mm, respectively. After the peak, the residual strength continued developing with the increase of the shear displacement until the test was finished. The peak shear strength obtained from the lab tests generally shows a good agreement with that predicted by Barton's formula. Under 1 MPa normal stress, the maximum difference between the lab test and Barton's formula is only 0.97%, while under the normal stresses of 0.4 MPa and 2 MPa, the differences are around 2.08% and 3.39%, respectively. The comparison shows a slight difference between the lab test results and Barton's equation. The possible source of difference may be due to the reproduction of the artificial joint with a given JRC. The above results also indicate that the artificially generated jointed specimen may be applied further in other physical model

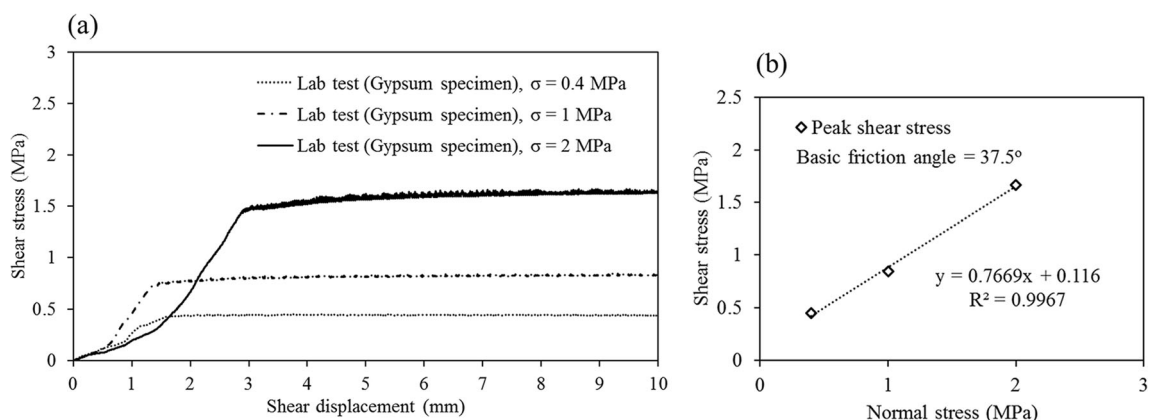


Fig. 4 The flat surface model: (a) the stress versus displacement curves under different normal stresses; (b) the determination of basic friction angle

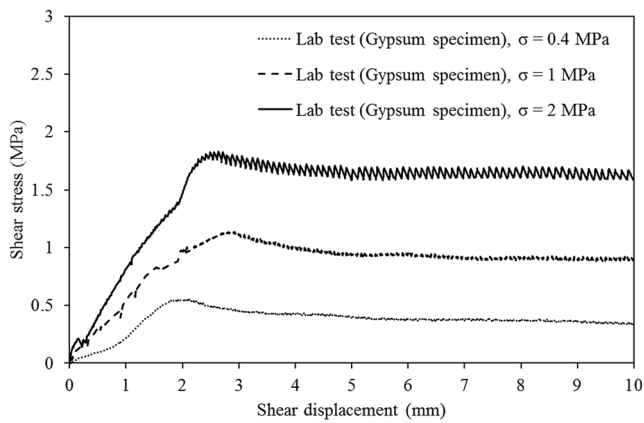


Fig. 5 DS test results for the gypsum model with the given JRC = 19.6 (scanned JRC: 16.8) under various normal stresses

tests that need actual joint profiles incorporated into the simulation.

Figures 6, 7, and 8 show the variation of the joint profiles with the JRC = 16.8 under various normal stresses after shearing. The value of the scanned JRC = 16.8 would be used in the following sections. In the laboratory, the damaged area of the joint profile, which was marked as the red-dashed line with a rectangular shape, was determined by visually comparing two joint profiles (one was before the test, and another was after the test). To investigate the influence of normal stress on the failure mechanism of a joint, a damage ratio, which was defined as the sheared area divided by the total area of the joint profile, was calculated. In Fig. 6, the damage ratio is about 15.85%, while the remaining parts almost retain the shape of the joint surface (84.15%). The result indicates that the residual shearing resistance mostly comes from the sliding between the lower and upper parts of the specimen. Therefore, under low normal stress (0.4 MPa), most of the shear strength of the rock joint may arise from the frictional resistance along the joint surface. The contribution of cohesion to the shear

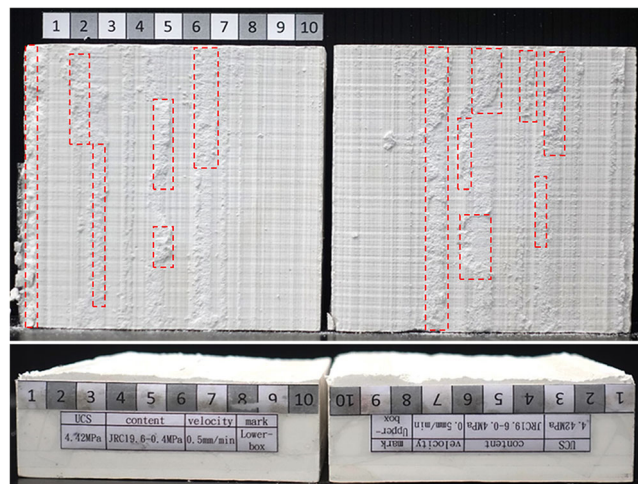


Fig. 6 Lower and upper sections of a gypsum plaster specimen under the normal stress of 0.4 MPa after shearing

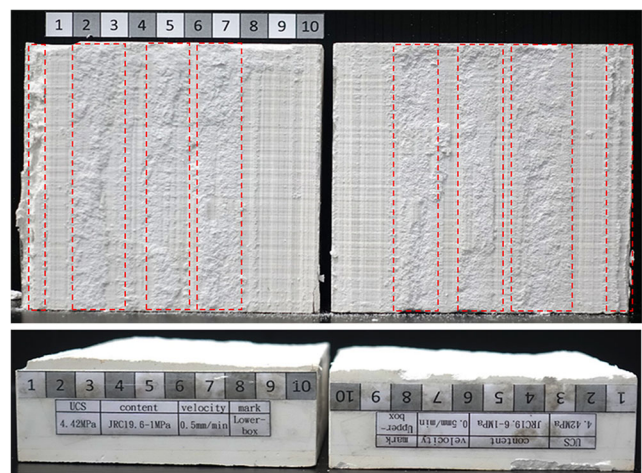


Fig. 7 Lower and upper sections of a gypsum plaster specimen under the normal stress of 1 MPa after shearing

strength of the joint is small. However, under high normal stresses (1 MPa and 2 MPa), the damage ratios increase considerably to 53.8% and 69.4% (Fig. 7 and Fig. 8), which implies that the joint profiles are damaged more severely than that under low normal stress. Hence, the frictional characteristics of the joint surface and part of the cohesion of the gypsum model may both partially contribute to the peak or residual shear strength of the specimen. The above findings prove that the failure mechanism of the joint profile strongly depends on the normal stress applied to the artificial gypsum specimen. However, this conclusion, which is based on the lab observation, only indicates the residual stage of the specimen. The source of the peak shear strength still cannot be clarified based on the final stage of the specimen. The result of lab tests may need to be checked with a result of the numerical simulation to figure out the source of the peak shear strength from a microscopic point of view.

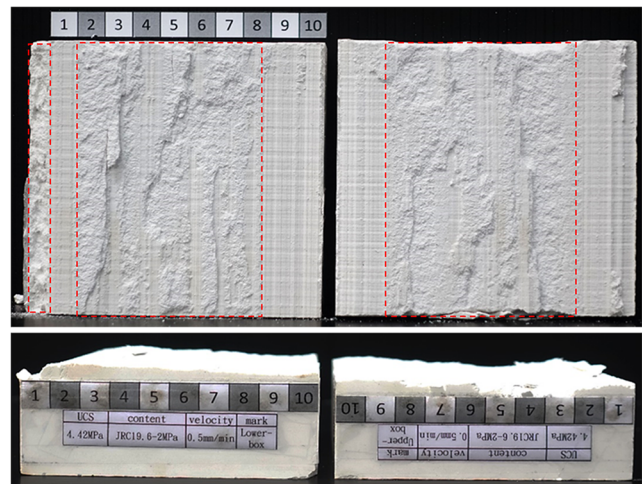


Fig. 8 Lower and upper sections of a gypsum plaster specimen under the normal stress of 2 MPa after shearing

Table 2 Parameters in the 2D-DEM model

Model	Particle property	Values
Linear contact	Effective modulus (N/m ²)	0.8×10^8
	Normal to shear stiffness ratio (-)	2.5
	Friction coefficient	0.7
Linear parallel bond	Bond effective modulus (N/m ²)	1.5×10^7
	Normal to shear stiffness ratio (-)	2.5
	Critical damping ratio (-)	0.05
	Tensile strength (Pa)	4.3×10^6
	Cohesion (Pa)	7.2×10^7
	Friction angle (°)	0
Smooth joint	Normal stiffness per unit area (N/m ³)	2×10^8
	Shear stiffness per unit area (N/m ³)	2×10^8
	Friction coefficient (-)	0.7

Formulation of the DEM model

DEM simulation was conducted for two types of tests, comprising the UCS test and DS test. The UCS of the gypsum specimen in the laboratory was determined as 4.42 MPa. The UCS model in 2D-DEM was then established by generating 112,045 connected particles with a uniform diameter of 0.25 mm using the linear model (Cundall 1979) and linear parallel bond model (Potyondy 2011). In the linear model, linear and dashpot components are established to simulate the behavior of an infinitesimal interface without resisting relative rotation or the zero contact moment. The linear component is used to present the linear elastic frictional behavior, while the dashpot component simulates viscous behavior. In the UCS simulation, the linear parallel bond model simulates the behavior of two interfaces. The first interface, which provides an infinitesimal (linear elastic and frictional interface), does not resist relative rotation and acts as the linear model. The second bonded interface, which provides a finite-size with the linear elastic, acts in parallel with the first interface and can resist relative rotation. The behavior of the second interface is linear elastic until the strength reaches the limit. When the bonding is broken, it makes the interface unbonded and carries no load. The unbonded linear parallel bond model now acts as the linear model. (Itasca Inc. 2017) The diameter

and the height of a UCS specimen, which was the same in both laboratory and numerical models, were 50 mm and 125 mm, respectively. The UCS test was simulated by moving the upper wall (upper plate) downward with a constant velocity of 0.021 mm/s (1% of the total height of specimen per minute), while the lower wall (lower plate) played a stationary role. The zero friction was installed between the particle assembly and walls during the test, while the critical damping ratio was set as 0.05. The nine micro-parameters in the DEM model were adjusted by performing trial and error in the UCS simulation. Once the UCS and the failure condition of the 2D-DEM model compared well with the result of the lab test, these micro-parameters (Table 2) could be chosen as the most suitable values for further simulation with the DS test.

Afterward, three DS models with the same particle bonding parameters as in the UCS ones were created following the dimension of the actual DS specimen in the laboratory (Fig. 9a). The length and height of the direct shear box, which was chosen to fit the artificial JRC profile length of 100 mm, were 100 mm and 70 mm, respectively. The particle size in the UCS model should be similar to that in the DS model because the same micro-mechanical properties of particle assembly are required. However, if the particle size of 0.25 mm (used in the UCS model) is adopted in the DS model, then the simulation may be terminated because it exceeds the computational limitations of the hardware. Therefore, three layers with two different particle diameters (0.5 mm and 0.25 mm) were generated, which was also proposed and suggested by Lê et al. 2018. A total of 31,084 particles with a diameter of 0.25 mm were generated at the middle layer; the lower and upper layers contained 23,845 particles with a diameter of 0.5 mm. The DS box consisted of a lower part (black walls), and an upper part (pink walls) was constructed as in Fig. 9b. The top wall with a servo-control function was applied to simulate the given normal stress on the top surface of the model. With a known coordinate of the joint profile (the dip angle of the joint orientation), the joint surface with JRC = 16.8 (the red line in the middle of the model in Fig. 9b) was formed using a smooth joint model, and its properties are also listed in Table 2. In this model, contacts between all particles along with two sides of the joint are assigned as built-in smooth-joint un-bonded with the normal stiffness, shear stiffness, and friction coefficient.

Fig. 9 The dimension of DS specimens with JRC = 16.8: (a) laboratory; (b) 2D-DEM model

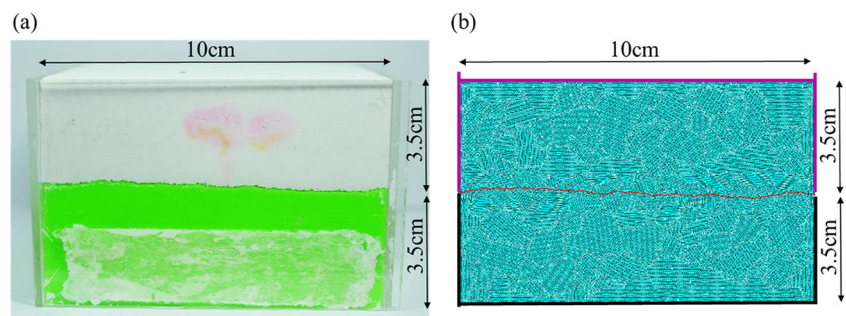
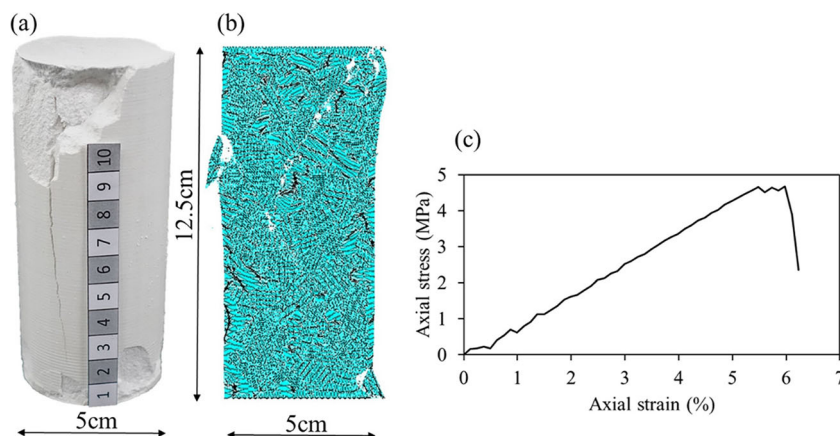


Fig. 10 Results of UCS test: (a) gypsum plaster specimen at failure, (b) simulated specimen at failure, (c) the stress-strain curve of UCS simulation



Therefore, the smooth-joint model can be used to simulate the relative sliding with dilation (or contraction) along with the joint interface. The influence of the particle shape can be neglected. The joint geometry, which can be fixed with respect to the global axes, contains a planar interface separating the two surfaces. The two contacting entities at the planar interface, which are defined as piece 1 and piece 2, will be related to the joint orientation change. The contact unit-normal vector is defined as the connection from the center of piece 1 to the center of piece 2. The smooth joint model (PFC-2D by Itasca Inc. 2017) can be modeled using force-displacement law. The accumulated normal and shear displacement can be continuously updated based on the gap value between the two pieces. Besides, the contact forces (including normal and shear forces), slip state, and bonding strength are updated based on the bonding status (if the model is bonded). In this study, the un-bonded smooth joint model is used. Therefore, when the shear force is updated, the slip state is also updated. If the slip state occurs, then the contact will be sliding. While slipping, shear displacements will cause an increase in normal force because of dilation. The increase of normal force strongly depends on the friction coefficient (μ), dilation angle (ψ), normal stiffness (k_n), and shear stiffness (k_s) of the joint. During shearing, if the shear stress exceeds the bonding

strength of the particle assembly, the parallel or normal bonds (linear parallel bond model) of particles, which are adjacent to the joint surface, are sheared to form the linear contacts (linear model). The input parameters for the smooth joint model were estimated based on a series of trials and errors in comparing the stress-strain curves between the 2D-DEM models and the lab tests under the same DS conditions.

The DS models were then analyzed by moving the lower part from left to right at a constant velocity of 0.5 mm/min. During the DS simulation, the built-in function measurement circles in 2D-DEM were installed along with the joint profile in the middle of a specimen to observe the change of shear stresses under various normal stresses (0.4 MPa, 1 MPa, 2 MPa), and at different shear displacements. Similarly, the distribution of contact forces amongst the particles was also plotted to compare with results obtained from the measurement circles. Besides, the number of broken bonds was continuously recorded to estimate the development of fractures during shearing. In 2D-DEM simulation, the distribution of contact forces can be visualized as the concentration of forces between particles, which is related to the variations of joint profiles and the direct shear micro-mechanical behaviors. The simulated direct shear specimen is to duplicate the mechanical behaviors of the jointed gypsum specimen. The mechanical

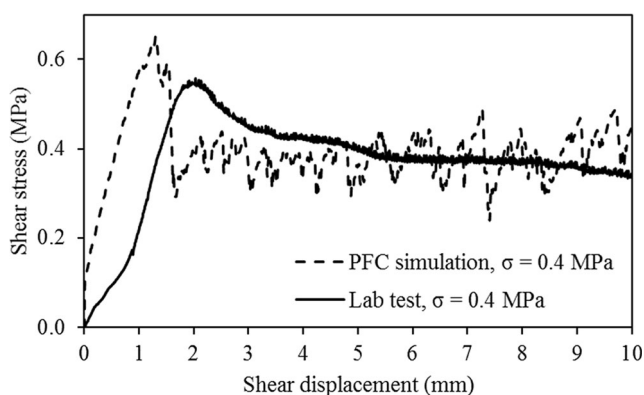


Fig. 11 Comparison of DS test results for the gypsum model and 2D-DEM model under normal stress of 0.4 MPa

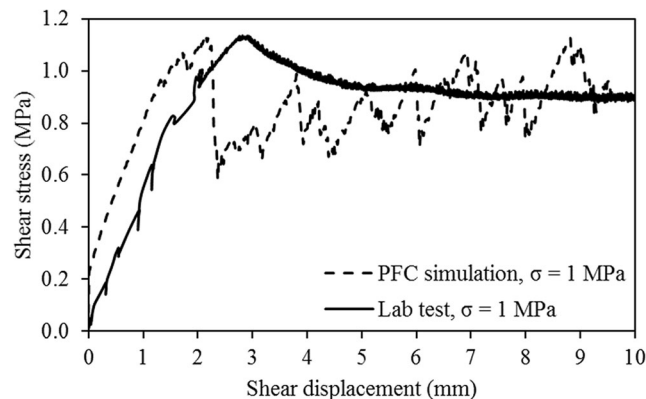


Fig. 12 Comparison of DS test results for the gypsum model and 2D-DEM model under normal stress of 1 MPa

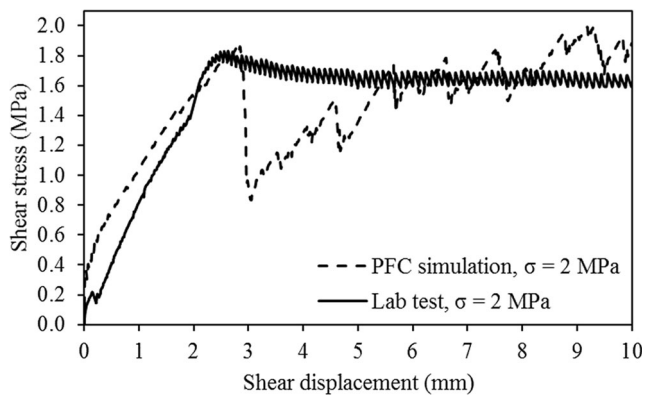


Fig. 13 Comparison of DS test results for the gypsum model and 2D-DEM model under normal stress of 2 MPa

behavior of the gypsum specimen is characterized by its cohesion and the friction angle. Therefore, the bonding and the frictional properties are given to the simulated specimen in 2D-DEM models. The bonding properties are further featured by tension and shear bonding. In the current study, we analyzed the percentage of broken bonds to explore how the shear strength was developing throughout the shearing process.

Direct shear simulation

Comparison between laboratory test and numerical simulation (including model validation)

In this study, a series of UCS tests in the laboratory and 2D-DEM simulation was conducted under stress-controlled conditions. The average UCS of the gypsum specimen was about 4.42 MPa. With given input parameters, the UCS of the 2D-DEM model was approximately 4.45 MPa, which was similar to the lab results. The failure condition of the gypsum specimen and 2D-DEM model after the test is also depicted in Fig. 10. One can observe that the same inclined cracks were formed in both two cases, with some slight differences. Figure 10c shows the typical axial stress-axial strain curve of the UCS in 2D-DEM simulation. In the laboratory, the stress-controlled equipment was used to obtain the UCS of

the gypsum mixture. Therefore, only the axial stress at failure was obtained with no stress-strain curve for comparing with the result of numerical simulation. However, the above results prove that the use of 2D-DEM to simulate the behavior of a gypsum plaster model is potential and acceptable. Hence, the same settings of input parameters were also applied to the DS models for further analyses.

Figures 11, 12, and 13 compare the DS results of the lab test and the numerical simulation under different shear displacements. The peak shear stresses obtained from the 2D-DEM models under the normal stresses of 0.4 MPa, 1 MPa, and 2 MPa are 0.65 MPa, 1.125 MPa, and 1.867 MPa, respectively. The difference in the peak shear strength between lab tests and numerical simulation is also presented in Table 1. The result shows that the peak shear strength of 2D-DEM models is almost similar to that in the laboratory, especially under the normal stresses of 1 MPa and 2 MPa, the differences were only 0.89% and 2.52%. Although the peak shear strength of the 2D-DEM model under the normal stress of 0.4 MPa is slightly higher than that of the lab test (the difference was about 13.85%), the slope of stress-strain curves (before the peak was reached) implies a similar trend in both two cases. The peak shear strengths of the two models (under the normal stress of 0.4 MPa and 1 MPa) are reached at the shear displacements of 1.3 mm, 2 mm, which is slightly different from the lab test. Conversely, the shear displacement (2.8 mm), where the peak strength is obtained, is almost similar to the lab test under the normal stress of 2 MPa. These slight differences may be due to the influence of two-dimensional models in 2D-DEM. From the observation of the joint surface in Figs. 6, 7, and 8, the damage is non-uniform along with the joint profile (in the horizontal direction perpendicular to the shearing direction), especially the specimen under the normal stress of 0.4 MPa. On the other hand, this behavior can not appear in 2D-DEM models because if the joint is damaged, it is then completely sheared. In this study, we performed a 2D analysis in both laboratory and numerical simulation. We expected that the artificially jointed gypsum specimen would be sheared and damaged in 2D condition, which was similar to the 2D-DEM model. However, after shearing, we found that some local parts of the joint profile were damaged in an

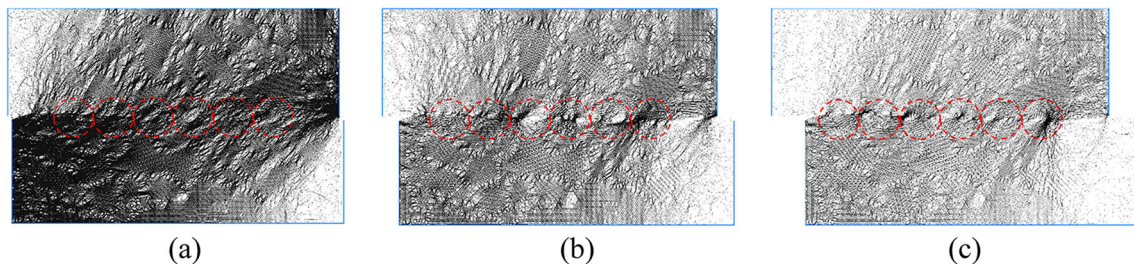


Fig. 14 Distribution of contact forces under the normal stress of 0.4 MPa at various shear displacements: (a) 1.3 mm; (b) 5 mm; (c) 10 mm. The maximum contact force was scaled to 6 kN

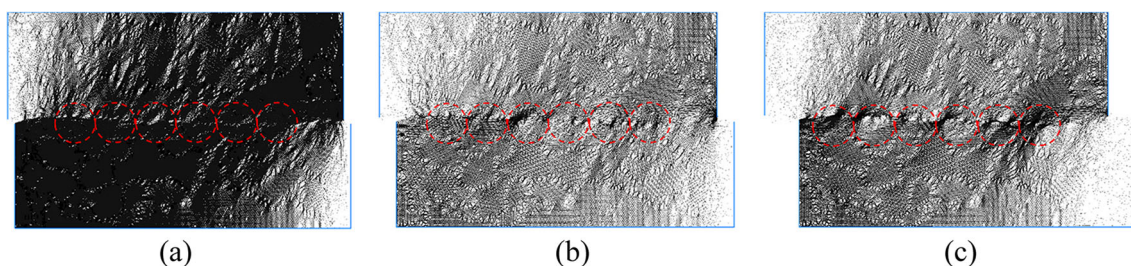


Fig. 15 Distribution of contact forces under the normal stress of 1 MPa at various shear displacements: (a) 2.16 mm; (b) 5 mm; (c) 10 mm. The maximum contact force was scaled to 6 kN

inconsistent way (3D behaviors). Therefore, for future research, the use of a 3D numerical model may need to be conducted to have a better comparison with the lab test results. Nonetheless, the residual shear strength of all 2D-DEM models shows a good agreement with the test data in the laboratory, which both exhibit slight strain-softening behavior. Therefore, the above outcomes indicate that the 2D-DEM simulation compares reasonably well with that from the lab test. Once the 2D-DEM model is validated, micromechanical behaviors of the joint profile during shearing can be discussed in more detail. In this study, we would like to discuss the so-called micromechanical behaviors in a DS specimen. However, the actual scale of mechanical behaviors that we explored falls in the grain-scale range because we are analyzing the forces and bonds between the particles and grains. In the DS test, we typically obtain shear strength parameters such as the cohesion and friction, which can be deemed as macro-mechanical parameters. Therefore, the exploration of the sources of the mechanical behaviors inside the jointed specimen may be termed as micro-mechanical behaviors.

Distribution of contact forces of DS models during shearing

The development of contact forces during shearing plays a vital role in understanding the micromechanical behavior of the joint rock profile. Figures 14, 15, and 16 illustrate the distribution of contact forces within the joint specimens at different shear displacements. Each chain of contact force is represented by a solid line between two adjacent particles. The

thickness of the line illustrates the magnitude of the normal contact force. In this study, the maximum value of the contact force inside the specimen under different normal stresses was scaled to the same amount of 6 kN for easier comparison. Under this setting, the influence of normal stresses on the distribution of contact forces can be observed and compared. The results indicate that the most extensive distribution of contact forces is observed at the shear displacement, where the peak shear strength is reached. This outcome is reasonable because, at this stage, the peak shear strength of the rock joint is completely mobilized. The distribution of contact force is non-uniform for various normal stress levels and at various shear displacements. At the stage of peak stress, most of the contact forces concentrate on the shear plane, and along with the joint profile. However, at 5-mm and 10-mm displacements, the distribution of contact force is smaller and concentrates locally at some parts of the joint profile where the local JRC is large.

Figures 17, 18, and 19 show the shear stress measured from six measurement circles at different locations along with the joint profile. The solid line, which connected the average shear strength measured from measurement circles, was drawn as a function of shear displacement. The dashed line illustrated a standard deviation of shear stress amongst measurement circles at different shear displacements. Before the peak shear strength is reached, the shear stress in all measurement circles shows a slight variation along with the joint profile. The standard deviations of shear stress under different normal stresses (0.4 MPa, 1 MPa, and 2 MPa) are smaller than 0.03 MPa, 0.05 MPa, and 0.1 MPa, respectively. However, at

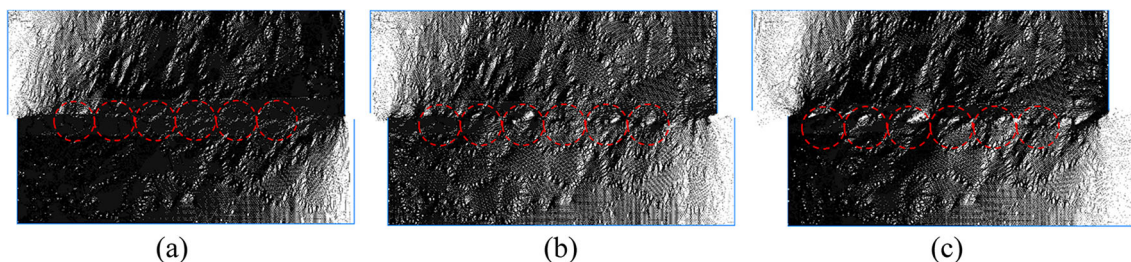
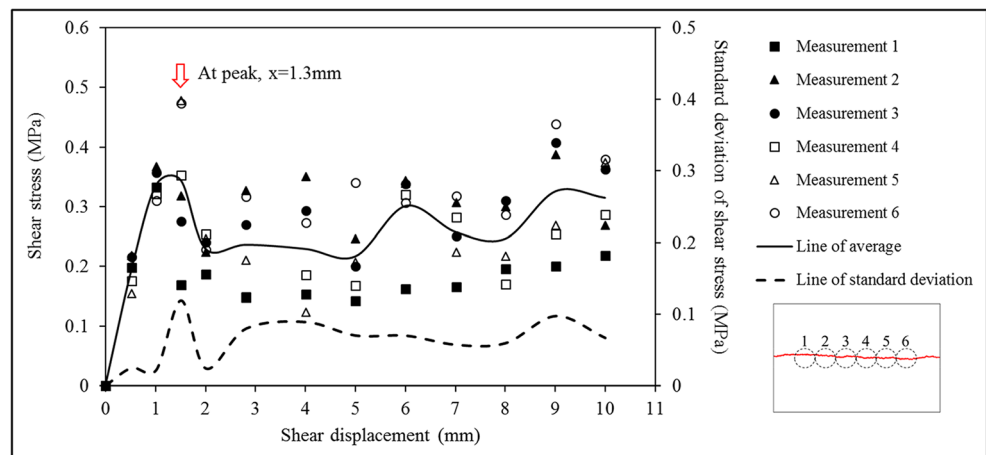


Fig. 16 Distribution of contact forces under the normal stress of 2 MPa at various shear displacements: (a) 2.81 mm; (b) 5 mm; (c) 10 mm. The maximum contact force was scaled to 6 kN

Fig. 17 Shear stress variations of six measurement circles under the normal stress of 0.4 MPa at various shear displacements



the residual stage, the shear stress significantly fluctuates amongst measurement circles; the standard deviation of shear stress shows a substantial increase in value. The variation of contact forces and shear stress may be attributed to the influence of the shearing process of the joint surface. After the peak shear stress is obtained, some local parts of the joint surface with large JRC values are sheared first and continue being sheared until the end of the test. The damage of a local joint may lead to the change of shear stress and contact forces at that location. The above results indicate that the distribution of contact forces and shear stress strongly depends on the local roughness of the joint profile and the applied normal stresses.

Development of fractures of DS models during shearing

Figure 20 shows the accumulation of fractures of the joint profile at different shear displacements. In the 2D-DEM model, the measurement circle is used to analyze the coordination number, porosity, stress, strain rate, and sizes of the particle assembly. However, the computation of the number of broken contacts is not provided within the measurement circles, see

PFC-2D (Itasca Inc. 2017). In this figure, the primary purpose of showing measurement circles is to illustrate their relative locations to the change of fracture development along with the joint profile. For the model under the normal stress of 0.4 MPa, the number of fractures is small and concentrates locally until the peak shear strength is reached. This result reveals that the peak shear strength of the joint model is mostly mobilized from the roughness of the upper and lower parts of the joint profile. However, at larger shear displacement (5 mm and 10 mm), more fractures are accumulated until the test is terminated. At this residual stage, some parts of the joint profile are completely sheared while the rest parts are still sliding to each other. This behavior was also observed on gypsum specimens after shearing in the laboratory (Figs. 6, 7, and 8). The above result indicates that the residual shear strength of the model may arise from both the reduced friction of the joint profile and the cohesion of the material (bonding strength of particles). The development of fractures for higher normal stresses (1 MPa and 2 MPa) shows a similar trend as in the 0.4 MPa case. The influenced zone of fractures was discussed by evaluating the width of such fractures. The maximum thicknesses of fractures at the end of the test (the shear

Fig. 18 Shear stress variations of six measurement circles under the normal stress of 1 MPa at various shear displacements

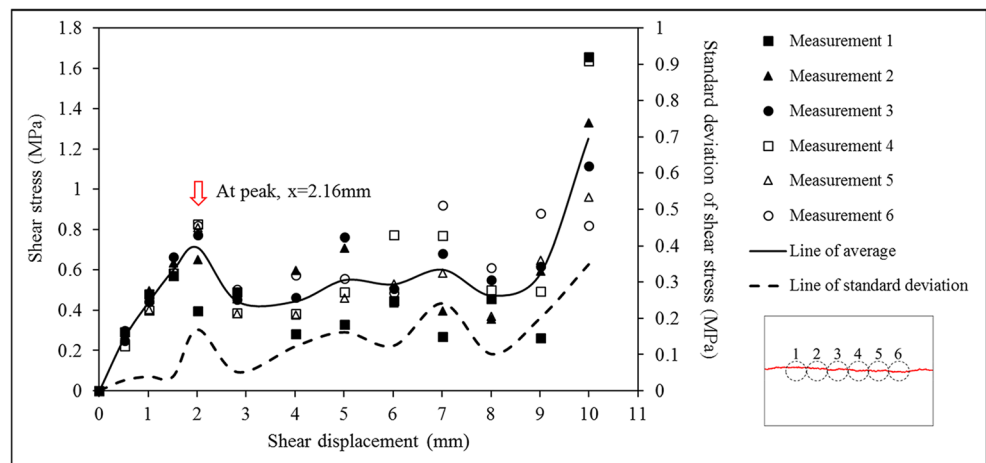
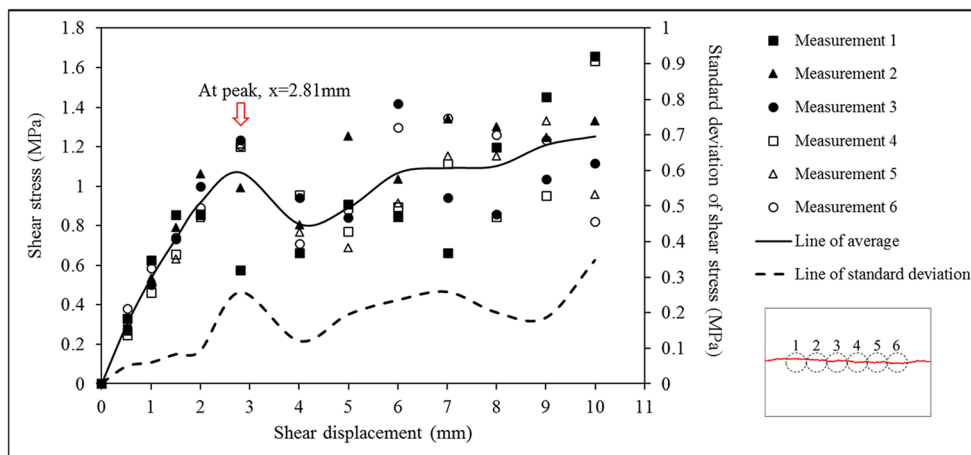


Fig. 19 Shear stress variations of six measurement circles under the normal stress of 2 MPa at various shear displacements



displacement of 10 mm) under various normal stresses of 0.4 MPa, 1 MPa, and 2 MPa are 1.13 mm, 1.18 mm, and 1.74 mm, respectively (Fig. 21). These results imply that the degree of normal stress has a significant impact on the development of fractures when the joint surface is sheared. The joint profile under high normal stress (2 MPa) is damaged more severely than that under low normal stresses (0.4 MPa and 1 MPa).

The development of fractures was also estimated by recording the number of broken bonds of the connected particles during shearing. Figure 22 illustrates the percentage of broken bonds as a function of shear displacement. Before the peak shear strength is reached, the number of broken bonds is close to 0% for the model with the normal stress of 0.4 MPa. Similarly, before the peak, the percentages of broken bonds for other normal stresses (1 MPa and 2 MPa) are recorded as small as 2.5% and 1.5%, respectively. The result from the number of broken bonds compares well with what analyzed in the development of fractures as aforementioned. The speed of developing fractures may also be evaluated using the slope of the curve in Fig. 22. The results reveal that at the same shear displacement, the bonds of particle assembly in the model

under high normal stress are broken much faster than that under intermediate and low normal stresses. Especially after the peak strength is obtained, the percentage of broken bonding increases sharply until the test is terminated. The maximum broken bonds for different normal stresses (0.4 MPa, 1 MPa, and 2 MPa) are 5.6%, 10.57%, and 13.89%, respectively; the highest value is observed under 2 MPa. The above discussion indicates that the failure mechanism of a joint during shearing is associated with normal stress applied to the model.

Conclusions

In this study, a series of DS tests with a given JRC were performed in both laboratory and 2D-DEM simulation. The joint profile with a JRC of 19.6 was generated using the PHV approach proposed by Lê et al. (2018). After the artificial gypsum specimen was replicated from the 3D-printed joint block, the actual JRC of the joint specimen was laser-scanned and determined as 16.8. Afterward, 2D-DEM was employed to simulate the joint model with the same actual

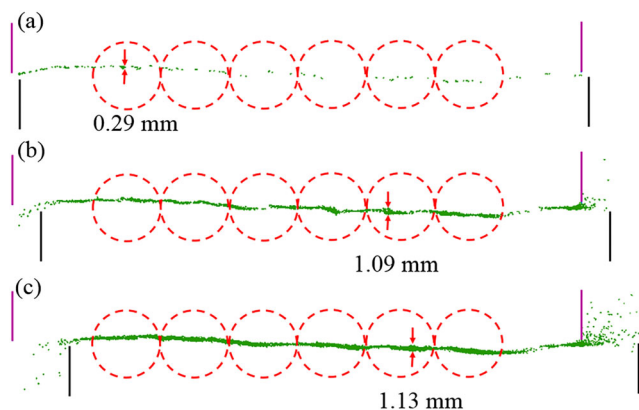


Fig. 20 Accumulation of broken bonds along with the joint profile under the normal stress of 0.4 MPa at various shear displacements: (a) 1.3 mm; (b) 5 mm; (c) 10 mm

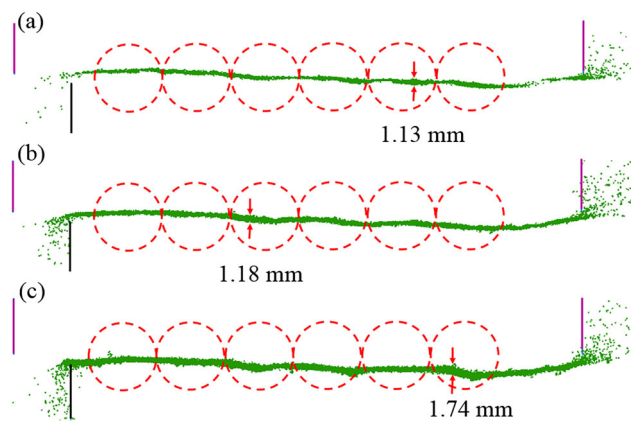


Fig. 21 Accumulation of broken bonds along with the joint profile at the end of the test under various normal stresses: (a) 0.4 MPa; (b) 1 MPa; (c) 2 MPa

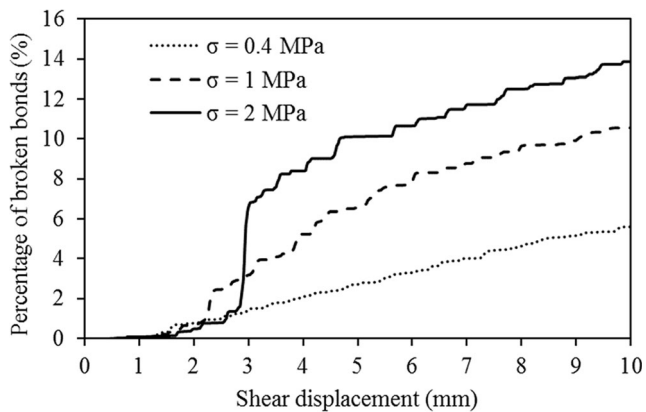


Fig. 22 Percentage of broken bonds of PFC model under various normal stresses during shearing

JRC as in the laboratory. The direct shear results from numerical simulation compared well with what were observed in the laboratory tests on gypsum plaster jointed specimens. The following conclusions could be drawn.

- (1) The peak shear strength of the simulated joint model with JRC = 16.8 compared well with that of the physical test under the same normal stress conditions, which indicated that 2D-DEM could be used to elucidate the micromechanical behaviors of the joint profile under the direct shear condition. Consistent results were also obtained by comparing laboratory test results and Barton's shear strength equation.
- (2) From a microscopic viewpoint, the distribution of contact forces was most concentrated at the early stage when the peak shear strength was reached. The distribution of shear stress along the shear plane was not uniform, depending on the degree of joint undulation and shear displacement.
- (3) In the laboratory, from the sheared surface of specimens after the test, we concluded that the friction and cohesion both contributed to the peak shear strength of gypsum specimen under intermediate and high normal stresses. However, this mechanical behavior might only be applicable in the residual stage of the shearing process because of the following observations from the microscopic point of view. The development of fractures in the 2D-DEM model showed that before the peak shear strength was reached, a few cracks were formed within the rock mass. However, as the shear displacement increased (at the residual stage), the number of cracks increased sharply and propagated into the rock mass. The degree of crack development was related to the normal stress level applied to the model; the higher the normal stress, the broader the influence zone of the fracture was observed.

The above results indicate that with a particular JCS (4.42 MPa in this study, i.e., a soft rock mass), the peak shear

strength of the jointed model (under different normal stresses) comes from the roughness along the joints with minimum damages of the joint surface. However, the residual strength arises from the reduced roughness and the shearing-off of the joints. The failure mechanism of the artificial joint model is correlated with the roughness of the joint (JRC), and the normal stress level applied.

- (4) Although the peak shear strength obtained in 2D-DEM was slightly different from that in lab test under the normal stress of 0.4 MPa (about 13.85% difference), most of the cases showed a good comparison in stress-strain curves and failure type. The results of this study demonstrate that the randomly generated profile can be applied to develop numerical and physical models for engineering purposes.

Funding The authors would like to thank the Ministry of Science and Technology of Taiwan, for financially supporting this research under contract MOST 107-2625-M-008-011 -.

References

- Bandis SC, Lumsden AC, Barton NR (1983) Fundamentals of rock joint deformation. *International Journal of Rock Mechanics and Mining Sciences & Geomechanics Abstracts* 20(6):249–268
- Barton N (1973) Review of a new shear-strength criterion for rock joints. *Eng Geol* 7(4):287–332
- Belem T, Homand-Etienne F, Souley M (2000) Quantitative parameters for rock joint surface roughness. *Rock Mech Rock Eng* 33(4):217–242
- Cheng C, Chen X, Zhang S (2016) Multi-peak deformation behavior of jointed rock mass under uniaxial compression: insight from particle flow modeling. *Eng Geol* 213:25–45
- P. A. Cundall, O.D.L.S., A discrete numerical model for granular assemblies. *Géotechnique*, 1979. 29(1): p. 47–65
- Fan, X., PHSW Kulatilake, and X. Chen, Mechanical behavior of rock-like jointed blocks with multi-non-persistent joints under uniaxial loading: a particle mechanics approach. *Eng Geol*, 2015. 190: p. 17–32
- Fereshtenejad S, Song J-J (2016) Fundamental study on applicability of powder-based 3D printer for physical modeling in rock mechanics. *Rock Mech Rock Eng* 49(6):2065–2074
- Huang W-C et al (2015) Micromechanical behavior of granular materials in direct shear modeling. *J Chin Inst Eng* 38
- Itasca Consulting Group Inc. 2017. Particle flow code in 2 dimensions (PFC2D version 5.0) – theory and background. Minneapolis, MN: Itasca Consulting Group
- Jing L, Nordlund E, Stephansson O (1992) An experimental study on the anisotropy and stress-dependency of the strength and deformability of rock joints. *International Journal of Rock Mechanics and Mining Sciences & Geomechanics Abstracts* 29(6):535–542
- Kana DD, Fox DJ, Hsiung SM (1996) Interlock/friction model for dynamic shear response in natural jointed rock. *International Journal of Rock Mechanics and Mining Sciences & Geomechanics Abstracts* 33(4):371–386
- Klinkenberg B (1994) A review of methods used to determine the fractal dimension of linear features. *Math Geol* 26(1):23–46

- Lê HK et al (2018) Spatial characteristics of rock joint profile roughness and mechanical behavior of a randomly generated rock joint. *Eng Geol* 245:97–105
- Le, H.K., Huang, W.C., Chien, C.C., 2019. Application of 3D-printing in generating artificial rock joint specimen with given JRC and its mechanical properties. *Proceedings of the 53rd US Rock Mechanics/Geomechanics Symposium*, New York, United States
- Lee YH et al (1990) The fractal dimension as a measure of the roughness of rock discontinuity profiles. *International Journal of Rock Mechanics and Mining Sciences & Geomechanics Abstracts* 27(6):453–464
- Liu Q, Xing W, Li Y (2014) Numerical built-in method for the nonlinear JRC/JCS model in rock joint. *The Scientific World Journal* 2014:7
- Liu Q et al (2017a) Updates to JRC-JCS model for estimating the peak shear strength of rock joints based on quantified surface description. *Eng Geol* 228:282–300
- Liu XG et al (2017b) Estimation of the joint roughness coefficient of rock joints by consideration of two-order asperity and its application in double-joint shear tests. *Eng Geol* 220:243–255
- Meng F et al (2018) Comparative study on dynamic shear behavior and failure mechanism of two types of granite joint. *Eng Geol* 245:356–369
- Myers NO (1962) Characterization of surface roughness. *Wear* 5(3):182–189
- Pickering C, Aydin A (2016) Modeling roughness of rock discontinuity surfaces: a signal analysis approach. *Rock Mech Rock Eng* 49(7):2959–2965
- Potyondy, D.O. “Parallel-bond refinements to match macroproperties of hard rock,” in *Continuum and distinct element numerical modeling in geomechanics 2011 (Proceedings of Second International FLAC/DEM Symposium, Melbourne, Australia, 14–16 (2011), pp. 459–465.*
- Tatone BSA, Grasselli G (2010) A new 2D discontinuity roughness parameter and its correlation with JRC. *Int J Rock Mech Min Sci* 47(8):1391–1400
- Wakabayashi N, Fukushige I (1992) Experimental study on the relation between fractal dimension and shear strength. in *Paper for the ISRM Symp. Fractured and Jointed Rock Masses. Lake Tahoe*
- Wang P et al (2017) Evaluation of the anisotropy and directionality of a jointed rock mass under numerical direct shear tests. *Eng Geol* 225:29–41